

COMPARISON BETWEEN THE POSITIVE SCHEMES AND WENO FOR HIGH MACH JETS IN 1D

YOUNGSOO HA

ABSTRACT. Comparison of high Mach number jets using positive schemes and Weighted ENO methods is considered in this paper. The positive scheme introduced by [11, 14] and Weighted ENO [9, 10] have allowed us to simulate very high Mach numbers more than Mach 80. Simulations at high Mach numbers and with radiative cooling are essential for achieving detailed agreement with astrophysical images.

1. Introduction

The astrophysical jets have been investigated in analyzing the physical mechanisms that rule their behavior to astrophysics. The images of the Hubble Space Telescope have led us to explain a new wealth of detail in gas flows and shock wave patterns involving astrophysical jets and colliding interstellar winds of particles. Simulating the astrophysical jets will allow us to explain the physical mechanisms that rule the fluid flows and shock wave patterns.

In this paper we model the HH 1-2 [8] astrophysical jets in one dimension, simulate its evolution numerically by means of the positive scheme introduced by [11, 14], and discuss the results compared with solutions using Weighted ENO (WENO-LF) methods [3, 9, 10] and exact. Since the HH 1-2 astrophysical jets are very high velocity mass flow the total energy is mainly composed of kinetic energy. High-order hyperbolic numerical methods developed over the last few decades perform well up to medium Mach numbers, but eventually produce negative pressures as the Mach number of the jet is increased. This makes the computing of the speed of the sound ($a = \sqrt{\gamma p / \rho}$) fail. And it yields the non-physical states. In order to simulate the HH 1-2 astrophysical jets or any other high Mach number jets, we need robust schemes to deal with intense radiative shocks in front of a bow shock.

Received July 10, 2006.

2000 *Mathematics Subject Classification.* 65M12.

Key words and phrases. positive schemes, WENO, conservative laws, euler equation.

Research supported in part by the BK21 project at KAIST.

The positive scheme allows us to simulate astrophysical jets with radiative cooling at very high Mach numbers - much higher than other methods. Computer simulations and astrophysical theory will allow us to analyze the detailed properties of astrophysical jet flows.

The modeled astrophysical jet in one-dimension has two shocks and a contact wave. We focus to explain the behavior of the positive scheme after simulating the astrophysical jet and discuss the accuracy of the positive scheme comparing with WENO-LF methods [3, 10] in the shocks and contact discontinuity. In section 2, we present the gas dynamic equations used to simulate the supersonic astrophysical jet. In section 3, we discuss briefly the positive scheme. In section 4, we compare the results obtained from the positive scheme and WENO-LF methods. Finally, in section 5, we draw conclusions.

2. Gas dynamic equations

In this section we consider the time-dependent Euler equation of gas dynamics. The Euler equation is a non-linear hyperbolic system of equations that simplify the Navier-Stokes equations by neglecting the effects of viscosity and heat conduction. From the mathematical point of view the Euler equation allows discontinuous solutions even if the initial conditions are continuous. Physically, the flow contains shocks or contact discontinuities. The Euler equation consists of equations for conservation of mass, momentum, and energy:

$$\begin{aligned}
 (1) \quad & \frac{\partial \rho}{\partial t} + \frac{\partial}{\partial x}(\rho u) = 0, \\
 (2) \quad & \frac{\partial}{\partial t}(\rho u) + \frac{\partial}{\partial x}(\rho u^2 + P) = 0, \\
 (3) \quad & \frac{\partial E}{\partial t} + \frac{\partial}{\partial x}(u(E + P)) = -n^2 \Lambda(T),
 \end{aligned}$$

where $\rho = m_H n$ is the density of the gas (predominantly H), $m_H = 938.272 \text{ MeV}/c^2$ is the mass of H, n is the number density, u is the velocity, ρu is the momentum density, $P = nk_B T$ is the pressure, k_B is Boltzmann's constant, T is the temperature, and

$$(4) \quad E = \frac{3}{2}nk_B T + \frac{1}{2}\rho u^2$$

is the energy density. The pressure is related to the internal energy density by the equation of state, which to an excellent approximation is polytropic:

$$(5) \quad P = (\gamma - 1)\left(E - \frac{1}{2}\rho u^2\right),$$

where the polytropic gas constant $\gamma = \frac{5}{3}$ for a monatomic gas like H.

Radiative cooling of the gas is incorporated through the right-hand side of equation (3), with the model for $\Lambda(T)$ taken from Fig.8 of Ref.[17]. The cooling

law can be modeled approximately by

$$(6) \quad \left(\frac{dE}{dt}\right)_{cooling} = -n^2\Lambda(T) \approx \begin{cases} -\tilde{\Lambda}(P^2 - P_a^2), & \text{if } T > T_a \\ 0 & \text{otherwise} \end{cases}$$

where $\tilde{\Lambda} = -8.776$ in our computational units, P_a is the ambient pressure, and T_a is the ambient temperature. Note that the approximate cooling law expression begins to diverge from the tabulated cooling law for $T > T_\star \sim 10^6 K$.

3. The numerical method

We will use a positive scheme for the supersonic astrophysical flow simulations. We have extended and adapted the code for simulating very high Mach number flows with radiative cooling. In order to handle the radiative cooling source term in the gas dynamics equation we tried two different methods: (1) a splitting method for an implicit treatment of cooling, (2) an unsplitting method for positive schemes with an explicit treatment of cooling (see [4, 21]). The computational results were virtually identical. In the splitting method, first we solve the homogeneous gas dynamics equation (with $\Lambda \equiv 0$), and then we update the energy density E by solving the ordinary differential equation (ODE)

$$(1) \quad \left(\frac{dE}{dt}\right)_{cooling} = -n^2\Lambda(T).$$

3.1. Conservation laws

We consider the general form of systems of conservation laws. Let Ω be an open subset of \mathfrak{R}^m , and let F be a smooth function from Ω into \mathfrak{R}^m . Then the general form of a system of conservation laws in one dimensional space is

$$(2) \quad \frac{\partial q}{\partial t} + \frac{\partial F(q)}{\partial x} = 0, \quad x = (x_1, x_2, \dots, x_m) \in \mathfrak{R}^m, t > 0$$

where $q = [q_1, q_2, \dots, q_m]^T$ and $F(q) = [f_1, f_2, \dots, f_m]^T$. Here q is the vector of conserved variables, and $F = F(q)$ is the vector of fluxes and each of its components f_i is a function of q . An equation of the form (2) is written in conservation form and is called a set of conservation laws. We shall be concerned with hyperbolic conservation laws (2).

The one-dimensional gas dynamic equation without cooling obeys the non-linear system conservation laws:

$$(3) \quad \frac{\partial U}{\partial t} + \frac{\partial}{\partial x}(F(U)) = 0$$

with

$$(4) \quad U = \begin{bmatrix} \rho \\ \rho u \\ E \end{bmatrix}, \quad F(U) = \begin{bmatrix} \rho u \\ \rho u^2 + p \\ u(E + p) \end{bmatrix}.$$

This can be written in the quasi-linear form

$$(5) \quad \frac{\partial U}{\partial t} + A(U) \frac{\partial U}{\partial x} = 0,$$

where $A(U) = F'(U)$ is the flux Jacobian matrix.

3.2. Positive schemes

We consider a two parameter family of second-order accurate positive schemes introduced in [11, 14]. Now we consider one-dimension hyperbolic systems of conservation laws:

$$(6) \quad \frac{\partial q}{\partial t} + \frac{\partial}{\partial x}(f(q)) = 0,$$

$$(7) \quad q(x, t^n) = \begin{cases} q_j^n & \text{if } x < x_{j+1/2} \\ q_{j+1}^n & \text{if } x > x_{j+1/2} \end{cases}.$$

We discretize the $x-t$ plane by choosing a mesh width $\Delta x_j = x_{j+1} - x_j$ with uniform intervals, and define the discrete points (x_j, t^n) by

$$(8) \quad x_j = j\Delta x, \quad j = \dots, -1, 0, 1, \dots$$

$$(9) \quad t^n = n\Delta t, \quad n = 0, 1, 2, \dots$$

And we define the mid-point:

$$(10) \quad x_{j+1/2} = x_j + \frac{1}{2}\Delta x = (j + \frac{1}{2})\Delta x.$$

Rather than the pointwise value q_j^n as an approximation to the value $q(x_j, t^n)$ we view it as an approximating average value of q over the given interval. We define a cell average of $q(x, t^n)$ by

$$(11) \quad \bar{q}_j^n \equiv \frac{1}{\Delta x} \int_{x_{j-1/2}}^{x_{j+1/2}} q(x, t^n) dx.$$

We adopt the semi-discrete formulation to solve the conservation laws (6). Discretize the conservation laws (6) to obtain

$$(12) \quad \frac{dq(x, t)}{dt} = -\frac{\partial f(q(x, t))}{\partial x} \approx -\frac{1}{\Delta x} [f(q(x_{j+1/2}, t)) - f(q(x_{j-1/2}, t))],$$

and

$$(13) \quad \frac{dq_j(t)}{dt} = -\frac{1}{\Delta x} (\hat{f}_{j+1/2} - \hat{f}_{j-1/2}) \equiv \mathcal{L}(q^n; j),$$

where $q_j(t)$ is the numerical approximation to the point value $q(x_j, t)$ and the numerical flux $\hat{f}_{j+1/2}$ approximates $h_{j+1/2} = h(x_{j+1/2})$ to a higher order with $h(x)$ defined by

$$(14) \quad f(q_j(x)) = \frac{1}{\Delta x} \int_{x_{j-1/2}}^{x_{j+1/2}} h(\xi) d\xi.$$

The numerical flux $\hat{f}_{j+1/2} = \hat{f}(q_{j-r}, \dots, q_{j+s})$ is required to satisfy the following conditions: (1) Lipschitz continuous in all arguments (2) Consistency with the physical flux. Then the solution to the conservative scheme will converge to a weak solution of (6), if it exists, by the Lax-Wendroff theorem [12]. For the time discretization, a TVD Runge-Kutta discretization introduced by Shu and Osher in [18, 19] is used. The time discretization is presented at the end of this section.

The basic idea of the positive scheme is combining a second order accurate scheme with numerical flux f^{acc} , with another dissipative scheme with numerical flux f^{diss} . Then using the flux limiter introduced in [1, 7], we obtain the numerical flux of the form

$$(15) \quad \hat{f} = f^{diss} + L(f^{acc} - f^{diss}),$$

where the flux limiter L is near the identity when the flow is smooth and near zero otherwise. In this way the positive scheme attains high-order accuracy in regions of smooth flow, and a sharp monotone resolution of shock waves. The numerical flux $\hat{f}_{j+1/2}$ in each coordinate direction was given by the following formula:

$$(16) \quad \hat{f}_{j+1/2} = \frac{f(q_{j+1}) + f(q_j)}{2} - \frac{1}{2}R[\alpha|\Lambda|(I - \Phi) + \beta\mu(I - \Psi)]R^{-1}(q_{j+1} - q_j),$$

where the matrix R , Φ , $|\Lambda|$, μ , and Ψ are defined below, and the adjustable parameters α and β satisfy $0 \leq \alpha \leq 1$ and $\alpha + \beta \geq 1$. This positive scheme makes use of Roe's scheme [16], with an "entropy fix" [6] which guarantees a nonzero diffusive term through the choice of μ and β . An advantage – and a disadvantage – of positive scheme is that they have many parameters which can be adjusted to obtain high resolution of different flows.

To apply the gas dynamic equation (3),(4) to the positive scheme (16) we need the characteristic decomposition procedure of it. Based on the values of q_j and q_{j+1} , a mean Jacobian $A_{j+1/2}$ is defined at the interface $x_{j+1/2}$. Here we use the Roe averaging method [15, 16] to apply the equations (16) in the codes. The Roe solver between states q_j and q_{j+1} is based on averaged states

$$(17) \quad \bar{u} = \frac{\sqrt{\rho_j}u_j + \sqrt{\rho_{j+1}}u_{j+1}}{\sqrt{\rho_j} + \sqrt{\rho_{j+1}}},$$

$$(18) \quad \bar{H} = \frac{\sqrt{\rho_j}H_j + \sqrt{\rho_{j+1}}H_{j+1}}{\sqrt{\rho_j} + \sqrt{\rho_{j+1}}},$$

$$(19) \quad \bar{a} = ((\gamma - 1)[\bar{H} - \frac{1}{2}\bar{u}^2])^{1/2}.$$

Here we use $\gamma = 5/3$ and H_j is the total enthalpy

$$(20) \quad H_j = \frac{E_j + p_j}{\rho_j}.$$

Write $A = R\Lambda R^{-1}$, where Λ is the matrix of eigenvalues of A and R consists of columns of the right eigenvectors associated with the eigenvalues. $|\Lambda| = \text{diag}(|\lambda_i|)$, $i = 1, \dots, m$, is a diagonal matrix whose entries are the absolute values of the eigenvalues λ_i of A . Each entry of the diagonal matrix $\mu = \text{diag}(\mu_i)$ satisfies $\mu_i \geq |\lambda_i|$. The matrices $\Phi = \text{diag}(\phi_i(\theta_i))$ and $\Psi = \text{diag}(\psi(\theta_i))$ have entries which are the limiter functions evaluated at the local solution, where θ_i is the ratio of the slope at the interface in the upwind direction to the slope at the current interface:

$$(21) \quad \theta_i = \frac{l_i(q_J - q_{J-1})}{l_i(q_j - q_{j-1})}, \quad J = \begin{cases} j-1 & \text{if } \lambda_i \geq 0 \\ j+1 & \text{otherwise} \end{cases}$$

for $i = 1, \dots, m$ and where l_i is the i th row of R^{-1} .

We use limiter function [20] satisfying the constraints

$$(22) \quad 0 \leq \phi_i(\theta), \frac{\phi_i(\theta)}{\theta} \leq 2, \phi_i(1) = 1$$

and

$$(23) \quad 0 \leq \psi(\theta), \frac{\psi(\theta)}{\theta} \leq 1, \psi(1) = 1.$$

Each ϕ_i can be a different limiter function, and ψ is the minmod limiter function. The CFL condition insuring the positivity of the scheme (13) and (16) is

$$\frac{\Delta t}{\Delta x} (\alpha \max_{k,j} |\lambda^k(q_j^n)| + \beta \max_{k,j} \mu^k(q_j^n)) \leq \frac{1}{2}.$$

To retain high-order accuracy in time without creating spurious oscillations, it is customary to use so-called TVD Runge-Kutta methods [18, 19] as the ODE solver. These methods employ a convex combination of forward Euler steps to advance the solution in time. They are especially designed to maintain the TVD property, i.e., ensure that the solution is total variation diminishing. The second-order method (RK2) reads:

$$\begin{aligned} q_j^{(1)} &= q_j^n + \Delta t \mathcal{L}(q_j^n), \\ q_j^{n+1} &= \frac{1}{2} q_j^n + \frac{1}{2} [q_j^{(1)} + \Delta t \mathcal{L}(q_j^{(1)})]. \end{aligned}$$

4. Numerical results

In this section we present numerical results using the positive scheme for the gas dynamical equations (1)-(3) with cooling and without cooling in one-dimension. To validate the positive scheme, we made comparisons of simulations of WENO-LF and exact solutions. We discuss the numerical results for the gas dynamical equations for the positive scheme and WENO-LF 3rd (WENO-LF3) and 5th order (WENO-LF5) methods at the velocity = 30.0 (Mach number 80). We solve the gas dynamical equations on $(x, t) \in [0, 2] \times [0, 0.06]$ where

TABLE 1. Parameters for the jets in HH 1-2

	jet	ambient
γ	5/3	5/3
ρ	500 H/cm ³	50 H/cm ³
u_j	300 km/s	0
T_j	1000 K	10,000 K
c_j	3.8km/s	12 km/s

the initial condition for the equations is given by

$$(24) \quad \begin{bmatrix} \rho \\ u \\ p \end{bmatrix} = \begin{bmatrix} 5.0 \\ 30 \\ 0.4127 \end{bmatrix} \text{ if } x \leq 0.1, \quad \begin{bmatrix} \rho \\ u \\ p \end{bmatrix} = \begin{bmatrix} 0.5 \\ 0 \\ 0.4127 \end{bmatrix} \text{ if } x > 0.1.$$

Boundary conditions are implemented by ghost points for the rest of the boundary.

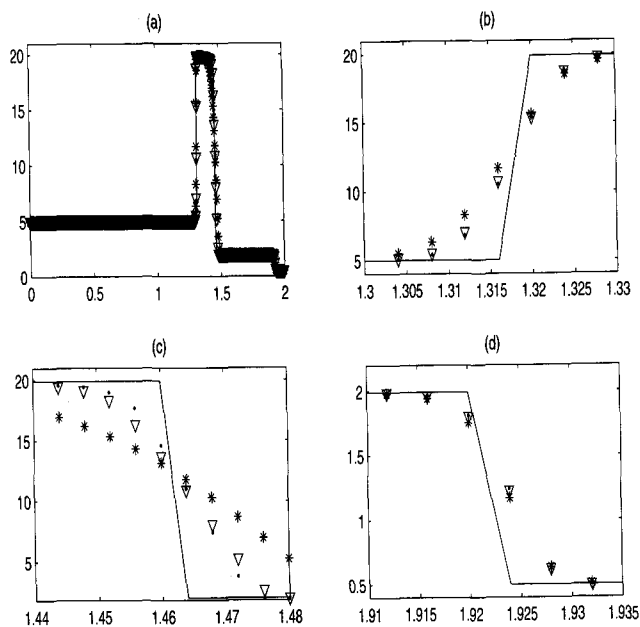


FIGURE 1. Results of Density without cooling at time $t=0.06$ with several parameters α and β ; (‘-’: exact, ‘.’: $\alpha=1.0, \beta=0.01$, ‘ ∇ ’: $\alpha=0.9, \beta=0.1$, ‘*’: $\alpha=0.5, \beta=0.5$) (b) second shock, (c) contact wave, and (d) first shock

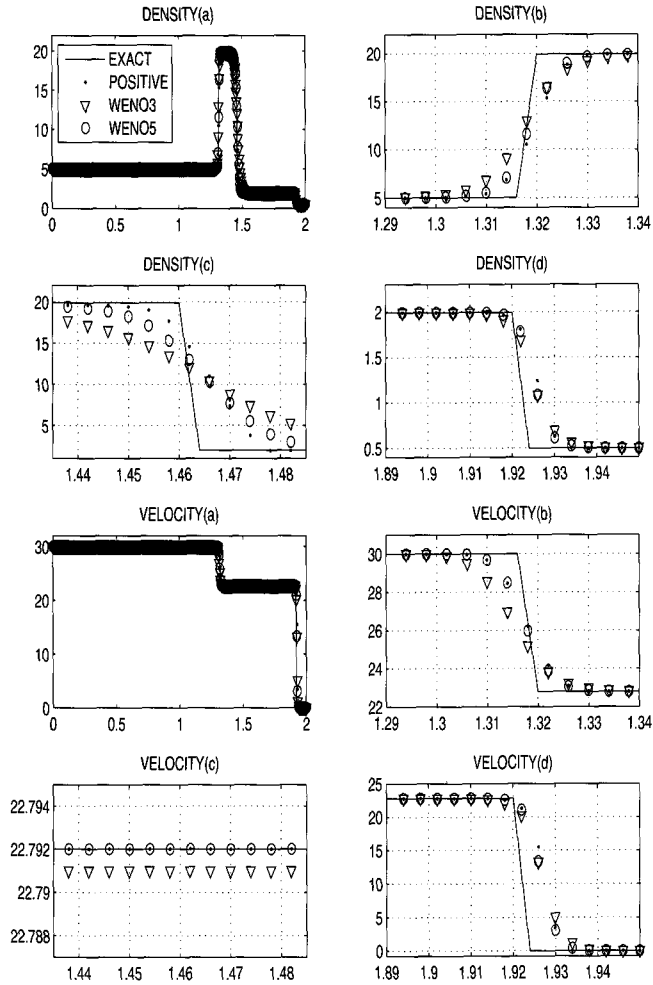


FIGURE 2. Jet for density and velocity without cooling at time $t = 0.06$, (b) second shock, (c) contact, and (d) first shock

The jets in HH 1-2 have the parameters listed in Table 1. The performances of the supersonic astrophysical jets without cooling are shown in Fig.1 - Fig.3 using 500 points ($\Delta x = 0.004$) with simulations using third- and fifth-order WENO-LF and with the exact solution. The parameters (α and β) and limiter

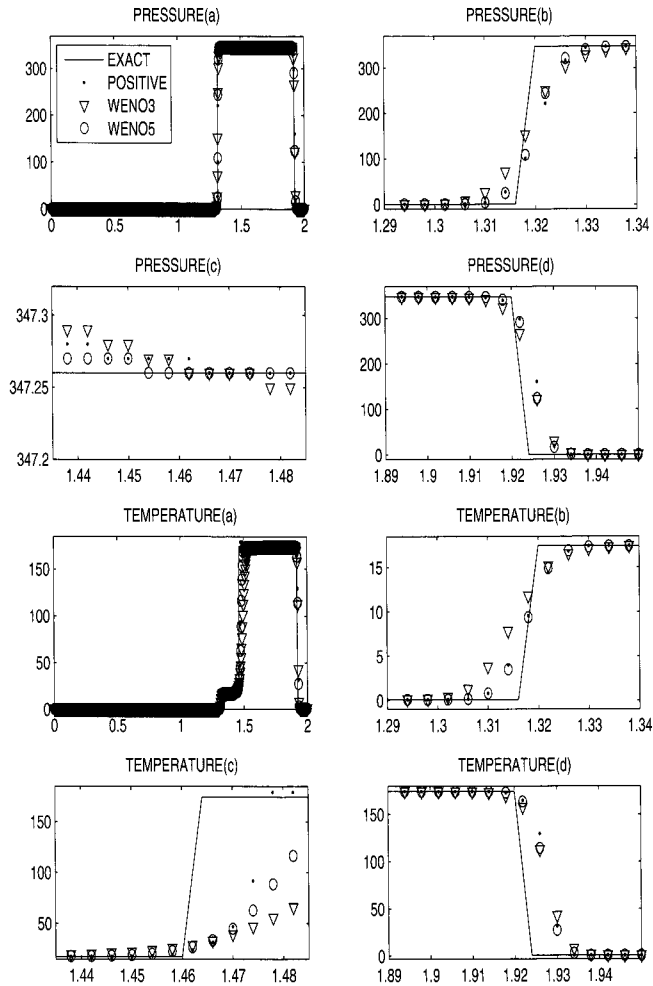


FIGURE 3. Jet for pressure and temperature without cooling at time $t= 0.06$ (b) second shock, (c) contact, and (d) first shock

functions are properly chosen for the positive scheme. Unfortunately we do not have a formula how to choose the parameters α and β but we can take the optimal values of the α and β by initial conditions or wave patterns. If a

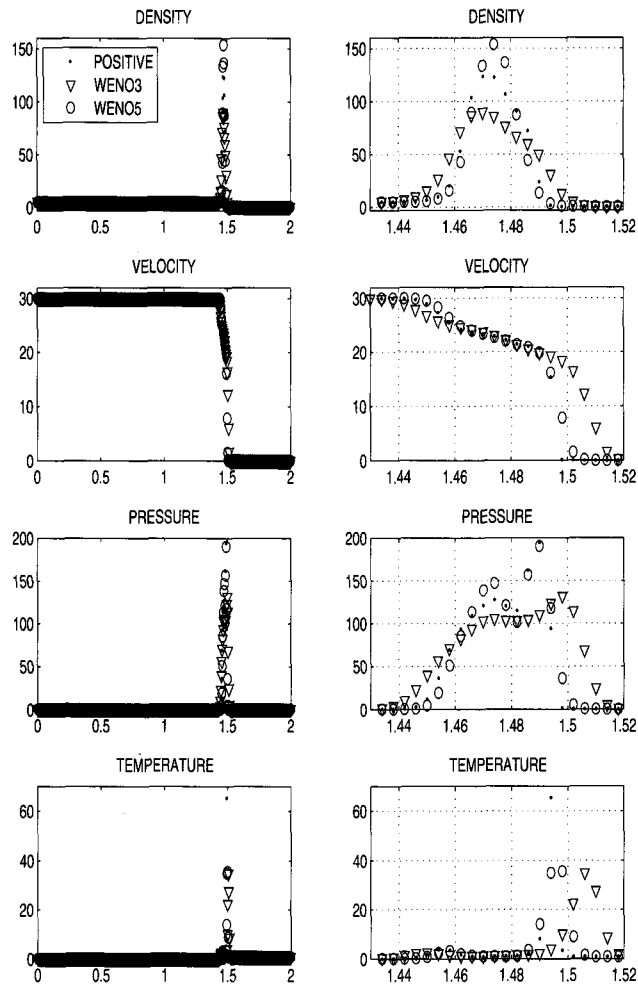


FIGURE 4. Jet with cooling at time $t = 0.06$, $\alpha = 1.0$, $\beta = 0.01$

solution of the equation consists of two symmetric rarefaction waves we need to take a smaller number α and a larger number β (test 2 in [21]). Indeed a larger number β leads to larger viscosity. Usually we chose closer 1 for α and 0 for β for the Euler equations whose solution consists with shock, contact, and

rarefaction waves. Since the solution of the jets has two shocks and a contact wave, we choose $\alpha = 1$ and $\beta = 0.01$. (see Fig.1).

If we are using the superbee limiter for $\phi_i(\theta_i)$ $i = 1, \dots, 3$, then the positive scheme yields negative pressure and can not compute the equation (16). To avoid negative pressure for the positive scheme we use the superbee limiter for $\phi_2(\theta_2)$ and Van Leer's function for $\phi_i(\theta_i)$ $i = 1, 3$ with adjustable parameters α and β . Fig. 2 and Fig. 3 have shown more detail of the solutions computed by the positive scheme, exact, and WENO-LF methods. The positive scheme and WENO-LF5 method perform virtually identically in the first and second shock waves. But the positive scheme produces a better result than WENO-LF5 on the contact wave. Indeed the WENO method has a weakness to compute the contact discontinuity.

The simulation (Fig. 4) with radiative cooling reproduces the morphology and physics of the cylindrically symmetrical jet in HH 1-2. Note the differences between the Mach 80 jet without and with radiative cooling. The jet with radiative cooling has a much higher density contrast near the jet tip (as the shocked, heated gas cools radiatively, it compresses) a much thinner bow shock, reduced Kelvin-Helmholtz rollup of the jet tip, and a lower average temperature. Radiative cooling is essential in understanding the density contrast and morphology of the jets and bow shocks in HH 1-2.

5. Conclusion

We simulated the HH 1-2 astrophysical jets using Euler gas dynamic equation with the positive scheme in 1-dimension. We compared the results of the positive scheme with those of WENO schemes in 1D. The positive scheme and WENO-LF are shown almost the same results for the first and second shock but the positive scheme has a better result for the contact wave (see DENSITY(c) in Fig.2 (c)) than WENO-LF5 for the Euler gas dynamic equation without cooling. Even though WENO-LF3 and WENO-LF5 are third and fifth order accuracy in space respectively, the WENO-LF5 is not better or almost the same accuracy as other second order numerical schemes (second order Godunov, central-upwind schemes, and several other schemes) solving the hyperbolic equation (2) (see [3, 4, 13]).

Since the modeling astrophysical jets have very high temperature and pressure with additional effects of radiative cooling we have to take circumspection about the negative pressure in numerical schemes. Fortunately the positive scheme by Liu and Lax [11, 14] gives us an excellent approximative results. We believe the simulation will help in analyzing the processes at work in the supersonic astrophysical jets. In order to make detailed simulations of the astrophysical images of the HH 1-2 jets including reproducing morphology, shock structure, and temperature/ionization profiles of both jets, as well as the pathological features of the asymmetrical jet, we plan to extend to 2 and 3

dimensional simulating the jet and the interaction of the jets with their ambient environments and to adapt the numerical code for a parallel version which is one of advantage of the positive scheme. There exists a trouble to apply WENO-LF5 for a 2 dimension astrophysical jet because of the dimple phenomenon in the bow shock. But since the positive scheme has flexible parameters and limiter function one may simulate the astrophysical jet in 2D and 3D using it. This is another advantage of the positive scheme.

References

- [1] J. P. Boris and D. L. Book, *Flux corrected transport I, SHASTA, A fluid transport algorithm that works*, J. Comput. Phys. **11** (1973), 38–69.
- [2] J. Gressier, P. Villedieu, and J.M. Moschetta, *Positivity of flux vector splitting schemes*, J. Comput. Phys. **155** (1999), 199–220.
- [3] Y. Ha, C. L. Gardner, A. Gelb, and C-W. Shu, *Numerical Simulation of High Mach Number Astrophysical Jets with Radiative Cooling* J. Sci. Comput. **24** (2005), 29–44
- [4] Y. Ha and Y. J. Kim, *Explicit solutions to a convection-reaction equation and defects of numerical schemes*, J. Comput. Phys. **220** (2006), 511–531.
- [5] A. Harten, P.D. Lax, and B. van Leer, *On upstream differencing and Godunov-type schemes for hyperbolic conservation laws*, SIAM Rev. **25** (1983), no. 1, 35–61.
- [6] A. Harten, *On a Class of High Resolution Total-Variation-Stable Finite-Difference Schemes*, SIAM J. Numer. Anal. **21** (1984), no. 1, 1–23.
- [7] A. Harten and G. Zwas, *Self-Adjusting Hybrid Schemes for Shock Computations*, J. Comput. Phys. **9** (1972) 568–583.
- [8] J. J. Hester, K. R. Stapelfeldt, and J. A. Scowen, *Hubble space telescope wide field planetary camera 2 observations of HH 1-2*, Astrophysical Journal **116** (1998), 372–395.
- [9] G-S. Jiang and C-C. Wu, *A High-Order WENO Finite Difference Scheme for the Equations of Ideal Magnetohydrodynamics*, J. Comput. Phys. **150** (1999), 561–594.
- [10] G-S. Jiang and C-W. Shu, *Efficient Implementation of Weighted ENO schemes*, J. Comput. Phys. **126** (1996), 202–228.
- [11] P. D. Lax and X.-D. Liu, *Solution of Two-Dimensional Riemann Problems of Gas Dynamics by Positive Schemes*, SIAM J.Sci.Comput. **19** (1998), no. 2, 319–340.
- [12] P. D. Lax and B. Wendroff, *Systems of conservation laws*, Commun. Pure Appl. Math. **13** (1960), 217–237.
- [13] R. Liska and B. Wendroff, *Comparison of Several Difference Schemes on 1D and 2D Test Problems for the Euler Equations*, SIAM J. Sci. Comput. **25** (2003), no. 3, 995–1017.
- [14] X.-D. LIU and P. D. LAX, *Positive Schemes for Solving Multi-dimensional Hyperbolic Systems of Conservation Laws*, J. Comp. Fluid Dynam. **5** (1996) 133–156.
- [15] R. J. LeVeque, *Numerical Methods for Conservation Laws*, Birkhauser Verlag, Basel (1992).
- [16] P. L. Roe, *Approximate Riemann solvers, parameter vectors, and difference schemes*, J. Comp. Phys. **43** (1981), 357–372.
- [17] T. Schmutzler and W. M. Tscharnuter, *Effective radiative cooling in optically thin plasmas*, Astronomy and Astrophysics **273** (1993), 318–330.
- [18] C.-W. Shu, *Total-variation-diminishing time discretizations*, SIAM J. Sci. Statist. Comput. **9** (1988), 1073–1084.
- [19] C.-W. Shu and S. Osher, *Efficient implementation of essentially non-oscillatory shock capturing schemes, II*, J. Comput. Phys. **83** (1989), 32–78.

- [20] P. K. Sweby, *High resolution schemes using flux limiters hyperbolic conservation laws*, SIAM J.Numer. Anal. **21** (1984), no. 5, 995-1011.
- [21] E. F. Toro, *Riemann Solvers and Numerical Methods for Fluid Dynamics*, Springer-Verlag, New York, 1997.

DEPARTMENT OF MATHEMATICAL SCIENCES
KAIST
TAEJON 305-701, KOREA
E-mail address: young@amath.kaist.ac.kr